



A review on autogenous self-healing behavior of ultra-high performance fiber reinforced concrete (UHPFRC)

Chao Yao^{1,2} · Aiqin Shen^{1,2} · Yinchuan Guo^{1,2} · Zhenghua Lyu^{1,2} · Ziming He^{1,2} · Hansong Wu^{1,2}

Received: 16 February 2022 / Revised: 19 April 2022 / Accepted: 29 April 2022 / Published online: 13 June 2022
© Wrocław University of Science and Technology 2022

Abstract

Ultra-high performance fiber reinforced concrete (UHPFRC) is well known for its superior workability, strength, ductility as well as durability, but its intrinsic self-healing ability is rarely valued and developed. This review focuses on the inherent potential or superiority, characterization, and mechanism of autogenous healing UHPFRC, aiming to obtain fundamental data for its mixture innovation, design, and application. High potentialities of autogenous self-healing UHPFRC depend on its excellent component requirements (fiber; abundant binding particles), mix design (high cementitious materials content, low water-binder ratio, moderate fiber content), rehydration capacity, and shrinkage or loading-initiated cracking features. Meantime, the generation of cracks makes the internal substances include active ingredients exposed to the external environment such as air, water, and temperature, which induces physical, chemical, and mechanical interaction between them at cracks. Intrinsic partial or entire sealing of the multiple cracks in UHPFRC has been proven to improve the safety and durability of UHPFRC infrastructures. A higher healing rate exists in cracks with a width of 75–175 μm , which is connected with crack healing kinetics, and the width of total healing cracks can reach up to 162 μm , which is mainly filled with calcium carbonate. Continuous accumulation of healing products at cracks can effectively improve the mechanical properties and suppress the decay of transport performance and steel fiber corrosion. Furthermore, mild fiber corrosion contributes to the partial restoration of flexural strength during the self-healing process.

Keywords Concrete · Ultra-high performance · Fiber · Crack · Self-healing · Recovery

1 Introduction

Ultra-high performance fiber reinforced concrete (UHPFRC), in recent years, has attracted widespread attention for its outstanding resistance to an external load and corrosive ions [1]. Its excellent workability, strength, ductility, energy absorption capacity, and durability are prone to promote a broader range of applications such as the containment of liquified natural gas [2], long-span bridges [3] as well as more slender concrete building components [4]. However, similar to ordinary concrete, a high cracking risk still exists for UHPFRC due to its brittleness, relatively low tensile

strength, and uneven shrinkage of internal composites [5]. Microcrack initiation allows harmful external ions to penetrate deeper inside the concrete. The coupling effects of water, temperature, and external loads induce rapid crack propagation of concrete, resulting in surface or structural damage, severe corrosion, poor mechanical properties and durability, and high maintenance cost. Thus, the cracks triggering a series of concrete deterioration are fundamental defects needed to be suppressed or solved.

Studies have reported that incorporating shrinkage-reducing admixture [5], chemical and mineral admixtures [6], fibers [7], and internal curing agents [8] can be used to inhibit concrete cracking, whereas concrete still has a high degree of cracking risk. In other words, cracking is currently an unavoidable problem for concrete. Meantime, the autonomous healing technologies of cement-based composite material self-repair technology can effectively heal micro-cracks [9], including the shape memory alloy embedded technology [10], electrodeposition technology [11], vascular technology [12], capsule technology [13], microbial technology [14]. Nevertheless, more effort is

✉ Chao Yao
yaochao@chd.edu.cn

¹ School of Highway, Chang'an University, South 2nd Ring Road Middle Section, Xi'an 710064, Shaanxi, China

² Key Laboratory for Special Area Highway Engineering of Ministry of Education, Chang'an University, South 2nd Ring Road Middle Section, Xi'an 710064, Shaanxi, China

needed to achieve a more straightforward production process, lower cost, mature products, and systematic evaluation.

In particular, the autogenous self-healing of concrete can be obtained based on the physicochemical reaction of the internal components. The self-healing ability can be significantly improved with the incorporation of mineral admixtures (fly ash (FA) [15], blast furnace slag [16], expansive materials [17], geo-materials [18], crystals and chemical additives [19]), multiple-scale fibers [20], nanofillers [21], and curing agents [22]. The improvement measures of self-healing are consistent with the direction of the traditional strength and durability improvement methods of concrete, characterizing its convenience, low cost, simplicity, and feasibility. It will bring inspiration to promote the inhibition of UHPFRC micro-cracks and better long-term performance.

UHPFRC characterizes its low water-binder (W/B) ratio, abundant cementitious materials, and an appropriate amount of fiber [23], following the requirement of high self-healing laws. High autogenous self-healing capability is proved with sufficient unreacted clinker or active calcium sources near the cracks [24, 25] and limited crack width [26, 27] for fiber-reinforced cementitious composites. In the meantime, many experimental characterizations have been carried out, proving that autogenous self-healing can restore mechanical properties [28] and durability [29]. The continuous or intermittent self-recovery will ultimately produce economic and environmental benefits due to the reduction of maintenance costs and increased service life.

Thus, the intrinsic self-healing of UHPFRC is potentially excellent due to the existence of fibers and various types of supplementary cementitious materials (SCMs) in the mixture proportion. Several studies have summarized its raw materials [30, 31], properties [32, 33], and applications [34]. However, a comprehensive assessment of the self-healing efficacy of UHPFRC is remained to be conducted for its special composition and cracking characteristics. More intelligent, durable, and sustainable UHPFRC matters with more practical designs of materials' compositions and suitable applications. This research focuses on the material composition, hydration, and cracking characteristics of UHPFRC in Sect. 2. Then, the self-healing effects on multi-scale structure, mechanical properties, and durability of UHPFRC under different exposure conditions were discussed in Sect. 3. Finally, the self-healing mechanisms of UHPFRC were reviewed in Sect. 4.

2 High potential of autogenous self-healing UHPFRC

2.1 Material characteristics

2.1.1 Raw materials

UHPFRC, e.g., ultra-high performance concrete (UHPC), is an ultra-high-strength and fiber-reinforced concrete produced from cementitious materials, fine aggregates, admixtures, steel fibers, or organic synthetic fibers, water, and other raw materials, which can be traced back to the mid-1990s [23]. Then, four basic principles are widely spread for producing UHPFRC: (a) Eliminating coarse aggregate to improve homogeneity; (b) Increasing compaction density by optimizing granular mixtures and applying pressure before solidification; (c) Strengthening the microstructure with heat treatment; (d) Incorporating fibers to enhance ductility [30, 32].

Therefore, the raw material composition of UHPFRC has some distinct characteristics based on the theoretical principles compared to other cement-based composites, such as engineered cementitious composite (ECC) and ordinary concrete. Table 1 presents the mixture proportion comparison among concrete, ECC, and UHPFRC. Generally, concrete consists of cement, water, fine aggregates, coarse aggregates, chemical additives, and mineral additives. As shown in Table 1, some apparent distinctions are the aggregate particle size distribution, used fiber type, and SCMs type among the three cement-based composites. Silica fume (SF) is considered an iconic element of UHPFRC [32, 35]. Fibers and water reducers are almost indispensable components of ECC and UHPFRC, but they are optional components for standard concrete components due to each performance requirement. Moreover, some ingredients can be partially or entirely replaced by other suitable materials for the three cement-based composites. For example, it is feasible to substitute cement or SF with abundant SCMs (such as granular blast furnace slag, FA, etc.) or fine mineral materials and reduce carbon footprint and price [32].

UHPFRC components are complex, but its typical components include binder materials (cement, SF, etc.), steel fiber, sand, water, and superplasticizer (SP) [32]. It has been reported that cement-based composites have a better self-healing ability due to the pozzolanic reaction of SCMs (including FA [35], slag [36]) and a better cracking restriction of fibers [37]. The limited crack width is easier to achieve complete closure during the self-healing process, so the existence of fibers and wide varieties SCMs will positively affect the autogenous self-healing of UHPFRC.

Table 1 Mixture proportion comparison among concrete, ECC, and UHPFRC

Types	W/B	Fiber	Aggregate		Cementitious material				SP	Ref
			Fine	Coarse	Cement	SF	Slag	FA		
UHPFRC	0.16	Steel	✓	×	✓	✓	×	×	✓	[29]
	0.17	Hybrid	✓	×	✓	×	×	×	✓	[38]
	0.18	Steel	✓	×	✓	×	✓	×	✓	[39]
	0.20	Steel	✓	×	✓	✓	×	×	✓	[40]
	0.18	Steel	✓	×	✓	✓	×	×	✓	[41]
	0.12	Steel	✓	×	✓	✓	×	×	✓	[42]
	0.15	PE	✓	×	✓	✓	×	×	✓	[43]
	0.22	Steel	✓	×	✓	✓	×	×	✓	[44]
	0.13	Steel	✓	×	✓	✓	×	×	✓	[45]
	0.22	Steel	✓	×	✓	✓	×	×	✓	[46]
	0.18	Steel	✓	×	✓	✓	×	×	✓	[47]
	0.16	H-steel	✓	×	✓	×	×	×	✓	[48]
	0.12	Steel	✓	×	✓	✓	×	×	✓	[49]
	0.15	Steel	✓	×	✓	✓	✓	×	✓	[50]
	ECC	0.27	PVA	✓	×	✓	×	×	✓	✓
0.27		PVA	✓	×	✓	×	✓	×	✓	[16]
0.16		PP	×	×	✓	×	×	✓	✓	[25]
0.20		PP	×	×	✓	×	×	✓	✓	[25]
0.30		PP	×	×	✓	×	×	✓	✓	[25]
0.30		PVA	✓	×	✓	×	×	✓	✓	[51]
0.27		PVA	✓	×	✓	×	×	✓	✓	[52]
0.21		PVA	✓	×	✓	×	×	✓	✓	[53]
Concrete	0.30	PE	✓	×	✓	✓	×	✓	✓	[54]
	0.40	/	✓	✓	✓	×	×	✓	✓	[8]
	0.50	/	✓	✓	✓	×	×	×	×	[55]
	0.40	/	✓	✓	✓	✓	×	×	✓	[56]
	0.35	/	✓	✓	✓	×	×	×	✓	[57]
	0.45	/	✓	✓	✓	×	×	×	✓	[58]
	0.45	Flax	✓	✓	✓	×	×	×	✓	[59]
	0.53	Cellulose	✓	✓	✓	×	×	×	×	[60]

“/” means no fiber, “✓” means the material is the composition of the mix, while “×” means the material is not the composition of the mix; Abbreviations: *PP* polypropylene, *PE* polyethylene, *H-steel* hybrid steel

2.1.2 Mix composition

Bulk density theory is one of the key theories for UHPFRC mix design. Larrard and Sedran [61] proposed one mortar type with a W/B of 0.14 and compressive strength of 236 MPa using a bulk density model based on the Mooney suspension viscosity model. After comparing some design methods, Mishra and Singh [62] clarified that the modified Andreason and Andersen model is one of the best methods for UHPFRC mix design. As shown in Table 1 and Fig. 1, to achieve reduced porosity, increased toughness, improved microstructure, and uniformity, the UHPFRC mix owns some basic requirements, including high cementitious material content, low W/B ratio, as well as a suitable amount of SP and fiber, excellent mixture design, and appropriate curing conditions.

Figure 1 also shows that UHPFRC has an appreciable binder material content, and the W/B ratio of UHPFRC is relatively lower than ECC, which is more evident than that of ordinary concrete. The realization of autogenous healing concrete requires sufficient un-hydrated particles and active calcium sources at the crack interface. Park and Choi [19] have demonstrated that unreacted clinker amount decreased with increasing W/B ratio, resulting in weaker autogenous healing performance. On the contrary, a smaller W/B can lead to an insufficient hydration reaction, leaving more unreacted clinker amounts in concrete mixes. Therefore, the UHPFRC system should have a considerable number of self-healing reactants.

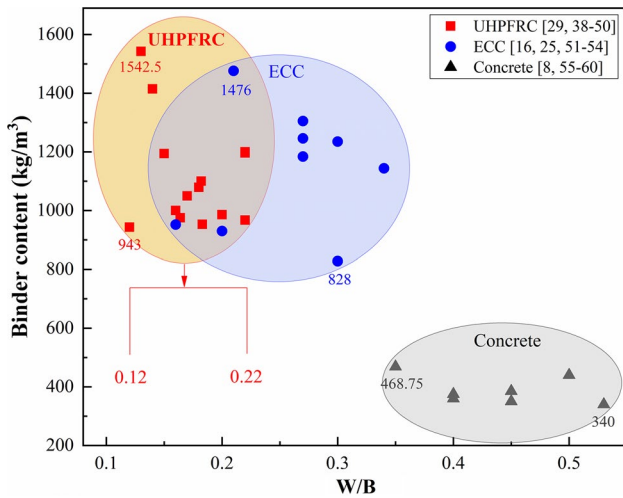


Fig. 1 Total binder content of UHPFRC [29, 38–50], ECC [16, 25, 51–54], and concrete [8, 55–60]

2.2 Hydration characteristics

The physical, chemical, or mechanical interaction between concrete itself and external substances or environments at the concrete cracks contributes to the self-healing of the cracks [63]. Chemical causes, including the rehydration of unreacted clinker, calcium carbonate formation, and pozzolanic reaction, are the critical aspect that contributes to the closure of cracks. The amount of the self-healing reactants, the content of unreacted minerals or active calcium hydroxide at the cracks, determines the potential of crack

healing. As the service time increases, the healing reactants will gradually decrease with the aging of the material. Thus, whether the material can continue to realize the self-healing of cracks during the service life is an issue of concern to researchers.

Figure 2 presents the rehydration test results and rehydration model of hardened UHPFRC matrixes. The determination of the degree of hydration (α_t) is calculated by Eq. (1) [64], where $W_n(t)$ and W_∞ are the non-evaporable water content at the rehydration time t (d) and full hydrated, respectively.

$$\alpha_t = W_n(t)/W_\infty \tag{1}$$

The W/B ratio for UHPFRC is about 0.12–0.22 (see Fig. 1). As shown in Fig. 2, the degree of hydration of hardened UHPFRC matrixes is low, basically less than 50%. Studies [24, 65] also demonstrated that the hardened UHPFRC involved large un-hydrated cement (50–60%). Mean-time, although the hydration of cement under appropriate conditions is continuous, accompanied by the constant consumption of un-hydrated clinker, the consumption of un-hydrated particles is limited (see Fig. 2), and only a certain amount of hydrated calcium silicate is stored during the process. Huang and Ye [66] show that the cement-based matrix with a 0.3 W/C ratio remains 30% un-hydrated cement after hydration for 42 days. Yildirim et al. [36] explored the autogenous self-healing capability of one-year-old ECC and found that cracks with a width of 458 μm can quickly be closed within 30 days. Therefore, it can be estimated that the self-healing potential of UHPFRC is enormous due to the considerable number of reactants for self-healing.

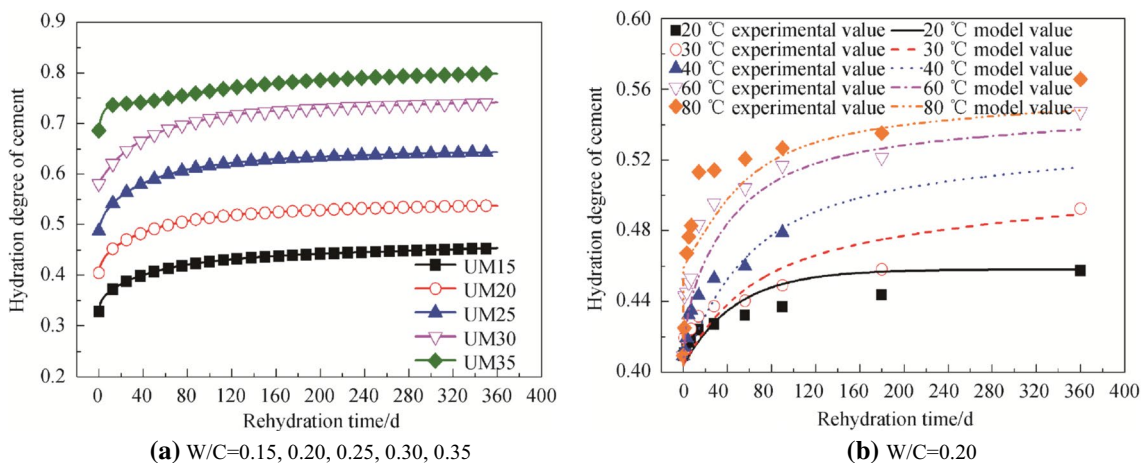


Fig. 2 Effects of a W/C ratio and b temperature on hydration degree of cement [64]

2.3 Cracking characteristics

2.3.1 Autogenous shrinkage cracking

The shrinkage properties of UHPFRC have been widely reported, including free and restrained shrinkage. The shrinkage can be mitigated by some measures such as incorporating expansive and shrinkage-reducing admixtures [67], employing a lower reinforcement ratio and the reinforcing bar with lower stiffness [68], using limestone filler [69]. Generally, shrinkage-induced cracks are hardly observed in shrinkage tests based on recent studies, which can be ascribed to the relaxation effect of UHPFRC [70, 71]. As reported in the literature, no visible shrinkage crack was observed in both the free and restrained shrinkage test [71]. However, the creep deformation was lower (about 60% of the free shrinkage deformations) in the restrained shrinkage test, resulting in high stress induced by shrinkage in the specimens after seven days of curing.

However, UHPFRC suffers from significant shrinkage due to its low water-to-binder ratio and high fine particle content, leading to a high potential for early cracking, especially for the decreased cross-sectional area of UHPFRC structures. For example, the free autogenous shrinkage magnitude of UHPFRC could reach 150 $\mu\text{m}/\text{m}$ at 48 h and 325 $\mu\text{m}/\text{m}$ at seven days [71]. Yoo et al. [70] found that the elastic stress of the ring UHPFRC samples was higher than the tensile strength. Hafiz et al. [69] also showed that the characteristic stress of UHPFRC under full restraint conditions could approach the ultimate strength. Yoo et al. [72] assessed the effects of thicknesses on the shrinkage of UHPFRC slabs. The tested width of cracks reached up to 0.2 mm and 0.04 mm for the UHPFRC slabs ($h=40$ mm) and UHPFRC slabs with 1% shrinkage-reducing admixture and 7.5% expansive admixture ($h=40$ mm) at seven days, respectively. It can be concluded that multiple cracks directly caused by shrinkage in UHPFRC are rarely observed, but high risks of cracking exist in UHPFRC structures, which are significantly affected by the material composition and shape type.

2.3.2 Load induced cracking

UHPFRC is a type of fiber-reinforced concrete, and its cracking behavior under loading depends mainly on the fiber content. For example, Wang and Guo [73] prepared three kinds of UHPFRC with three-volume fractions of steel fibers, i.e., 1.5% (Strain-softening), 2.0% (Low strain-hardening), and 2.5% (High strain-hardening). Based on the ultimate tensile hardening strain level, the MCS-EPFL recommendation divides UHPFRC into three categories: UO (strain softening), UA (strain hardening), and UB (high strain hardening) [41]. In more detail, the UHPFRC can be categorized into deflection softening or crack controlling with minor

enhancement, deflection hardening, tensile strain hardening, and high energy absorbing [74], representing different uniaxial tensile stress–strain relationships and equivalent bending stress–deformation behavior.

Thus, each type of UHPFRC has different crack characteristics, such as crack width, crack depth, initiation time, and corresponding load level, which have a conspicuous impact on self-healing ability and value evaluation of self-healing. Wang and Guo [73] studied the damage evolution process and crack width development of strain-softening UHPFRC, low strain-hardening UHPFRC, and high strain-hardening UHPFRC during the direct tensile test. Results indicated that high strain-hardening UHPFRC exhibited higher ductility and smaller crack width. Equivalent deformation is achieved by forming more cracks, i.e., a post-crack pattern with multiple microcracks for UHPFRC. Although the microcracks (less than 0.01 mm) are still generated when the strain is below 600 μe , the width of multiple microcracks is limited (typically below 0.05 mm) in the strain hardening stage. As shown in Fig. 3, Guo et al. [41] compared the cracking characteristics of high strain hardening UHPFRC and ECC. The cracks are invisible in the strain hardening stage, whose width is smaller than ECC.

Moreover, UHPFRC is often used in combination with steel bars. The yield strain of steel bars is about 0.2%. The crack width of high strain hardening UHPFRC was only 0.02–0.03 mm when tensile strain reached 0.2% [75, 76]. However, the crack width of strain-softening UHPFRC reached 0.5 mm [41]. Figure 4 presented the typical crack evolution of glass fiber-reinforced polymer (GFRP) bar-reinforced UHPFRC (with 2% steel fiber) beam [75]. The structure had cracked under the allowable load (≤ 60 kN), then the number of micro-cracks increased for the higher

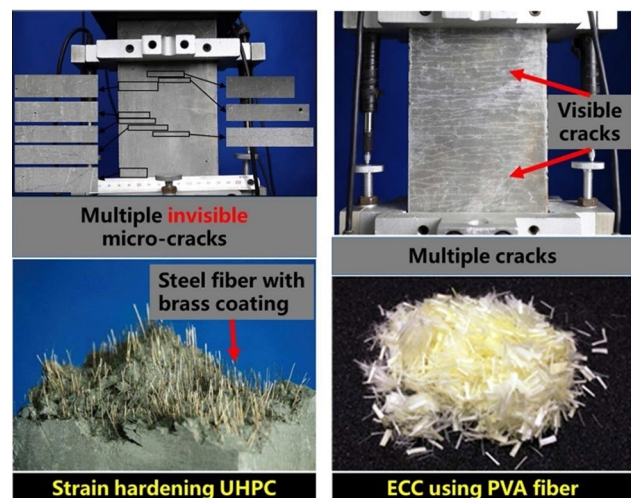


Fig. 3 Comparison between high strain hardening UHPFRC and ECC [41]

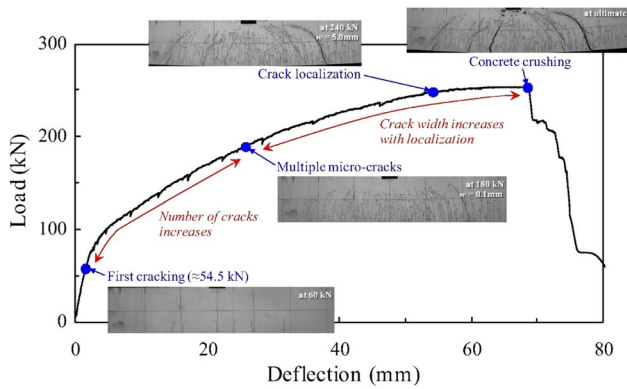


Fig. 4 Typical load–deflection response of glass fiber-reinforced polymer bar-reinforced UHPFRC (Fiber content = 2%) beam [75]

load, resulting in the decreased flexural stiffness. After that, the width of cracks gradually increased after about 70% of the peak load (180 kN). Notably, the crack width under a load of 180 kN is more than 0.1 mm. Moreover, considering the fatigue load’s characteristics, self-healing will have more time or opportunities to suppress the damage caused by cracks during the service period. Other studies also studied the relationship between crack width and loads, such as the rebar-reinforced UHPFRC beam [77] and steel-UHPFRC composite [76]. The crack width is within 0.05 mm for different structures at 20–100 kN. In general, the micro-cracks ($\leq 10 \mu\text{m}$) emerge in the early period under a relatively low load. The width of multiple cracks is restricted to 0.5 mm, or even 0.09–0.14 mm under the ultimate capacity state. It can be seen that the crack width increases significantly with the increase of the external load, but under the action of a considerable external load, the crack width is limited (0–0.5 mm), and a superior restriction on the crack width exists in the high strain hardening UHPFRC structures.

3 Autogenous self-healing behaviors of UHPFRC

Cracks will gradually be filled with self-healing products, which generally contribute to recovering mechanical properties and durability. Comparison analysis of the microstructure (particularly cracks), mechanical properties, and durability of specimens with or without healing are widely applied to assess self-healing efficiency. Thus, this section mainly reviews the behaviors of UHPFRC in the process of self-healing from three aspects: cracks, mechanical properties, and durability.

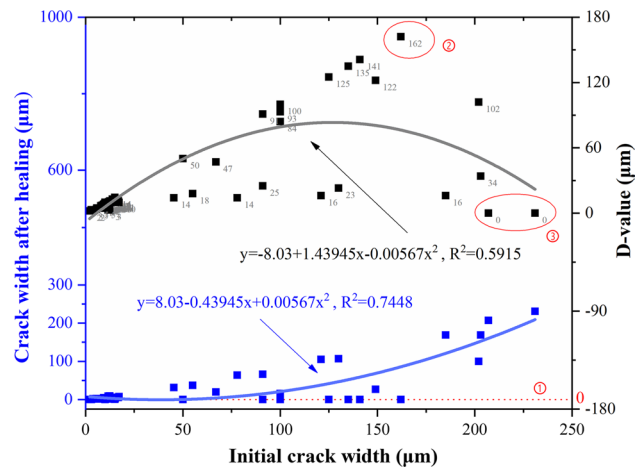


Fig. 5 Crack width of UHPFRC before and after self-healing [2, 10, 23, 28, 39]

3.1 Effects of self-healing on multi-scale cracks of UHPFRC

3.1.1 Evolution of multi-scale cracks for self-healing

Multiple micro-cracks appearing in concrete is one of the most intuitive signs of material damage, and more severe crack damages (higher number, deeper depth, larger width, and area) mean increased sensitivity to external factors such as load and erosion ions. In turn, the closure of multi-scale cracks contributes to the recovery of concrete properties [39]. Previous studies mostly used the evolution of crack width during the re-curing process to assess the self-healing ability.

As shown in Fig. 5, the crack width data of cracked UHPFRC before and after self-healing for some time and their difference value (*D*-value, see Eq. (2)) are collected from the related literature [2, 10, 23, 28, 39].

$$D\text{-value} = w_0 - w_t, \tag{2}$$

$$\text{Crack healing rate CHR} = D\text{-value}/t, \tag{3}$$

$$\text{Index of crack healing ICH} = (1 - w_t/w_0) \cdot 100\%, \tag{4}$$

where w_0 is crack width before self-healing, w_t is crack width at re-curing time t . Cracks with larger widths require more material to achieve complete filling.

In general, the crack width increases with increasing initial crack width after healing. However, the measured data are different from the law due to the influence of crack width on the self-healing rate, differences in environmental conditions, and the self-healing time effect. For example, the *D*-value reached up to 162 μm after 168 days re-curing

However, an extensive width makes it difficult to fully use the calcium ions transmitted from the matrix. The first reason possibly is that the calcium ions can hardly effectively exist on the surface of the crack. At the same time, a wide crack is generally accompanied by an enormous depth. Effective formation of healing products is hard to achieve at a considerable depth due to a lack of contact with the external CO₂, which has been confirmed by the research [81]. It indicates that it is not scientific enough to only use the crack surface width before and after healing to evaluate the degree of multi-scale self-healing. Moreover, the active calcium ions at the crack gradually decrease with the increasing self-healing time, and the new layer formed with self-healing products on the crack surface may slow down the diffusion transport of external CO₂ and water, which leads to a decrease in the self-healing rate.

3.2 Effects of self-healing on mechanical properties

3.2.1 Material and environmental impact on mechanical restoration

The pre-cracking method is commonly adopted to prepare specimens for assessing the healing capacity of UHPFRC, including the four-point bending test, direct tensile test, uniaxial tensile test, and three points bending test. Then, cyclic loading is applied to pre-cracked UHPFRC specimens under different re-curing times, and the impacts of healing on the mechanical properties are assessed by comparing the indices extracted from stress–strain curves among the

post-cracking specimens after re-curing, sound, and pre-cracking samples of UHPFRC. For example, Fig. 8 shows the direct tensile stress–strain curves corresponding to specimens being loaded and reloaded after 28 days of re-curing [41]. As shown in Fig. 8, no AE sources were detected till the tensile strain reached 0.009% and 0.011% during the second loading for the specimens re-cured in water, and the pre-cracking sample obtained partial restoration on the first cracking stress (4–5 MPa) during the self-healing process. Meantime, in the research [41], the recovery of the first cracking stress is only about 1–2 MPa and 0–0.5 MPa under 80% RH and 45% RH of re-curing condition, respectively. It can be concluded that the pre-cracking sample obtained mechanical recovery during the self-healing process based on the comparison of the first cracking stress of the sample at a different stage.

Table 2 further describes the variation of parameters of mechanical properties due to the self-healing effect such as strength, stiffness, ductility, toughness, and related derived indices. Under the impact of self-healing, some mechanical properties of cracked UHPFRC can be completely restored, even exceeding the original sample. For example, Kim et al. [2] reported that the self-healing ratio of post-cracking strength in the same group of samples was tested as 0.99, 1.00, 1.04, 1.15, and that of deflection capacity of the cracked UHPFRC reached up to 1.05, 1.07, 1.18, 1.23 with 28-days water curing process.

However, the degree of self-healing is unstable and variable due to the complex self-healing process. Many factors can affect it, including material compositions and exposure

Fig. 8 Tensile stress–strain curves and their relevant AE sources distribution of the specimens re-cured in water for 28 days [41]

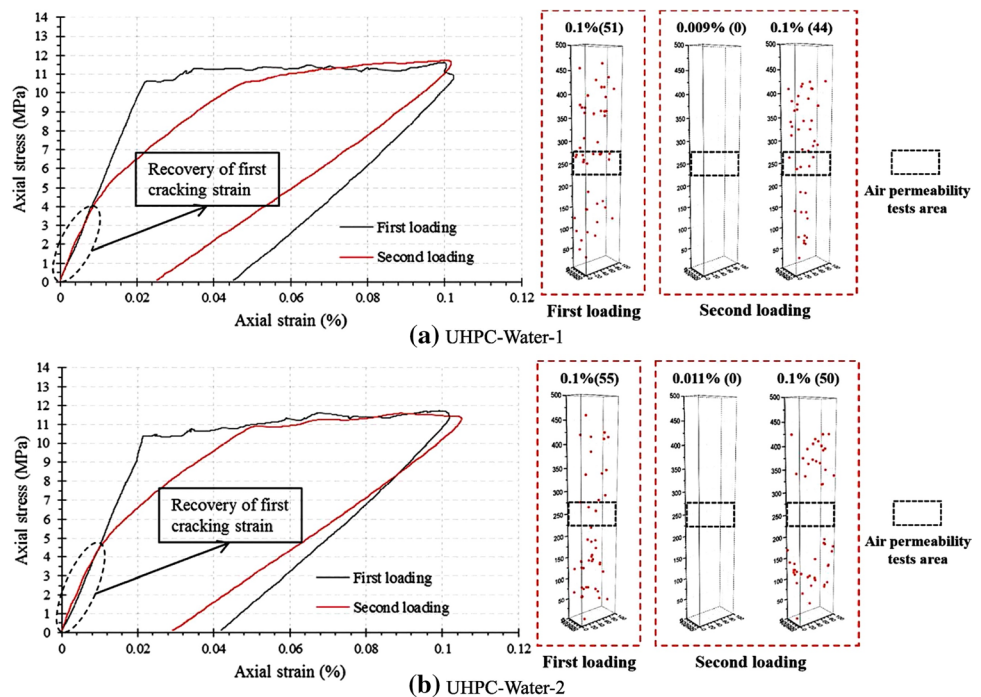


Table 2 Influences of self-healing on mechanical properties of UHPFRC

Ref.	W/B	Re-curing (age, d)	Indicators	Tested value
[23]	0.20	NS curing (0, 28, 70, 140)	(a) Tensile strength, MPa (b) Strain capacity, %	(17.3, 16.9, 17.6, 18.8) (0.65, 0.80, 0.82, 0.85)
[2]	0.20	CC + 3 days Air curing	(a) SFR of post-cracking strength, % (b) SFR of deflection capacity, % (c) SFR of toughness, %	(1.20); (1.02); (0.92); (0.98) (1.18); (0.92); (1.06); (0.94) (1.40); (0.92); (1.00); (0.94)
		CC + 28 days water curing	(a) SFR of post-cracking strength, % (b) SFR of deflection capacity, % (c) SFR of toughness, %	(1.15); (1.04); (1.00); (0.99) (1.18); (1.05); (1.23); (1.07) (1.36); (1.06); (1.24); (1.04)
[41]	0.18	28 days water curing; 28 days 80%RH curing; 28 days 45%RH curing	(a) Cracking strain recovery, % (b) Stiffness recovery, %	43.5 (water); 16 (80%); 0 (45%) 97.5 (water); 66 (80%); 46 (45%)
[65]	0.20	Water curing	(a) Stiffness	See Fig. 9
[24]	0.20	Water (0-S, 7, 21, 42, 70) Water (0-S, 0-C, 7, 21, 42, 70)	(a) Stiffness, kN/mm (b) Flexural resonance frequency (kHz)	(0.307, 0.209, 0.283, 0.301, 0.306) (1.59, 1.53, 1.58, 1.59, 1.59, 1.58)

NS NaCl solution, CC cryogenic cooling, 0-S sound sample without re-curing, 0-C cracked sample without re-curing, SFR self-healing ratio

environment. Some adjustments to material compositions of UHPFRC can achieve superior healing ability, such as increasing fiber content, incorporating a crystalline admixture [29], using alumina nanofibers [39]. Kim et al. [2] conducted a comparative analysis of the influence of five-type fiber on the recovery of flexural performance. Results indicated that longer or straight steel fibers used in UHPFRC could promote a higher self-healing capacity than shorter or twisted steel fibers. Notably, the experimental results displayed that the fiber type has a more significant impact on self-healing properties than the curing condition in the literature [2]. Thus, extensive research is needed to reveal the internal influence mechanism of different types of fibers, as well as of fiber thickness, length, surface condition, etc., on the self-healing process.

Many studies have been carried out to investigate the impact of re-curing conditions on the recovery of mechanical properties for UHPFRC. A comparative analysis of the effects of different re-curing conditions on the mechanical properties of UHPFRC was described in the literature [28]. Water supplies play a fundamental role in autogenous healing. Among different exposure conditions (immersed in water, exposed to air with low or high humidity, under wet and dry cycles), the specimens immersed in water showed faster and higher load-bearing capacity and stiffness healing. In contrast, self-healing was rarely observed or tested in the samples exposed to low humidity air. Compared to curing in water, Guo et al. [41] proposed a more effective method as the recovery of first cracking strain, tensile stiffness, and penetration resistance was more effective and less time-consuming for the samples under steam re-curing. Yoo et al. [23] found that though the tensile ductility of the plain UHPFRC sample increased after a period of exposure to

sodium chloride (NaCl) solution, the effect of self-healing resulted in a better tensile performance (such as the tensile strength and strain capacity) as compared to the plain sample. In particular, cryogenic cooling can contribute to unintended abrupt self-healing, and the cracked UHPFRC exposure to water showed better healing than air curing after exposure to cryogenic cooling [2]. On the whole, for curing conditions, the presence of water in the re-curing environment plays a crucial role in promoting self-healing, but the influence of ambient temperature and external chemical components (H_2CO_3 , NaCl, etc.) cannot be ignored.

3.2.2 Time-dependent effect on the recovery of mechanical properties

The self-recovery of mechanical properties is time-dependent, and it can be explained by the mechanisms of autogenous healing concrete [63] and the kinetics of self-healing (see Sect. 3.1.2). Figure 9 shows that the tested stiffness value of pre-cracking samples slowly recovered over time, exceeding the health specimens' value. As a whole, the healing efficiency is high at the beginning of the cracking and slowly slows down in the later stage.

However, some mechanical properties can only achieve partial or slight recovery reported in many studies, including the peak load of the three points bending test [65], the first cracking strain of the direct tensile test [41], the tensile strength, strain capacity, and g -value [23]. The restoration of mechanical properties can be explained by the bridge and filling effects of new crystals between the two sides of the cracks [65] and the increased interfacial bond between the steel fiber and matrix during the self-healing process [23]. However, on the whole, the short-term self-healing process

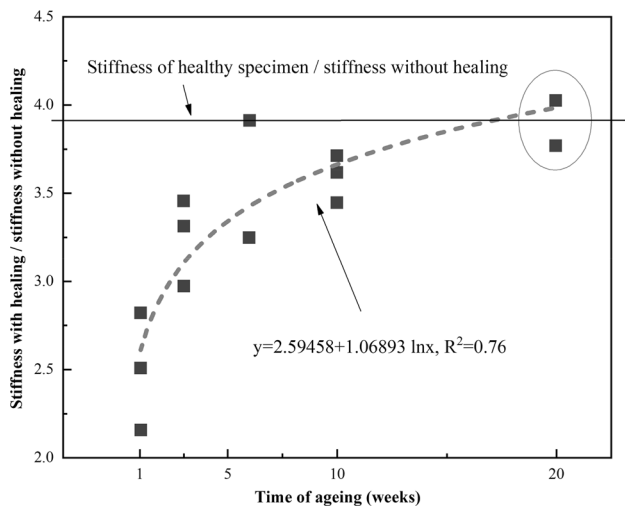


Fig. 9 Evolution of the ratio between the reloading stiffness with healing (in water) and the reloading stiffness without healing, as a function of aging, compared with the average stiffness of healthy specimens. [65]

of UHPFRC alone is not enough to make these crystals and new interfacial bond strength attain equivalent strength as the intact part. Nevertheless, partial or complete restoration of some mechanical properties is beneficial to resist external loads, and the existence of self-healing can make UHPFRC have a better long-term mechanical property. Therefore, how to increase the rate of self-healing, reducing the duration of self-healing, and improving the performance of self-healing products, as well as the bonding between self-healing products and the original concrete matrix, will become the future development direction.

3.3 Effects of self-healing on durability

The durability of UHPFRC includes many indicators, e.g., freezing resistance, impermeability, and corrosion. This part mainly focuses on the influence of autogenous healing on transport properties (i.e., gas, water, and chloride permeability) and corrosion based on the relevant literature.

3.3.1 Gas permeability

Permeability is one of the essential microstructural properties directly related to its durability and long-term performance. The gas permeability test, a non-destructive method, is widely used to assess concrete's pore structure and compactness. The gas (oxygen, nitrogen, or dry air) permeability measurements mainly include the CemBureau method, Torrent method, and OPI method for concrete [82]. Thus, previous studies adopted these methods to evaluate the self-healing effect on the gas penetration resistance of UHPFRC

based on the results of the gas permeability test between the pre-cracking samples and the self-healed samples.

It is a widely received viewpoint that the cracks will be gradually filled with self-healing products during the self-healing process. Then, the resistance to gas permeation will increase. Figure 10 shows the effects of the sample location, cyclic loading, re-curing condition, and time on the air permeability index [41]. The cyclic loading resulted in multiple declines of transport properties, which the AE analysis has confirmed. On the contrary, a longer self-healing in higher water content of the environment and a higher content of fiber [107] contributed to the improvement of the impermeability of UHPFRC. In more detail, Kwon et al. [83] reported the time dependence of air permeability of cracked UHPFRC during the self-healing process. The resistance to air penetration improved dramatically in the first three days. Then the recovery speed slowed down. Therefore, in a suitable environment, the self-healing effect of UHPFRC can continuously improve the gas permeability resistance, which has a positive effect on improving the durability and long-term performance of UHPFRC.

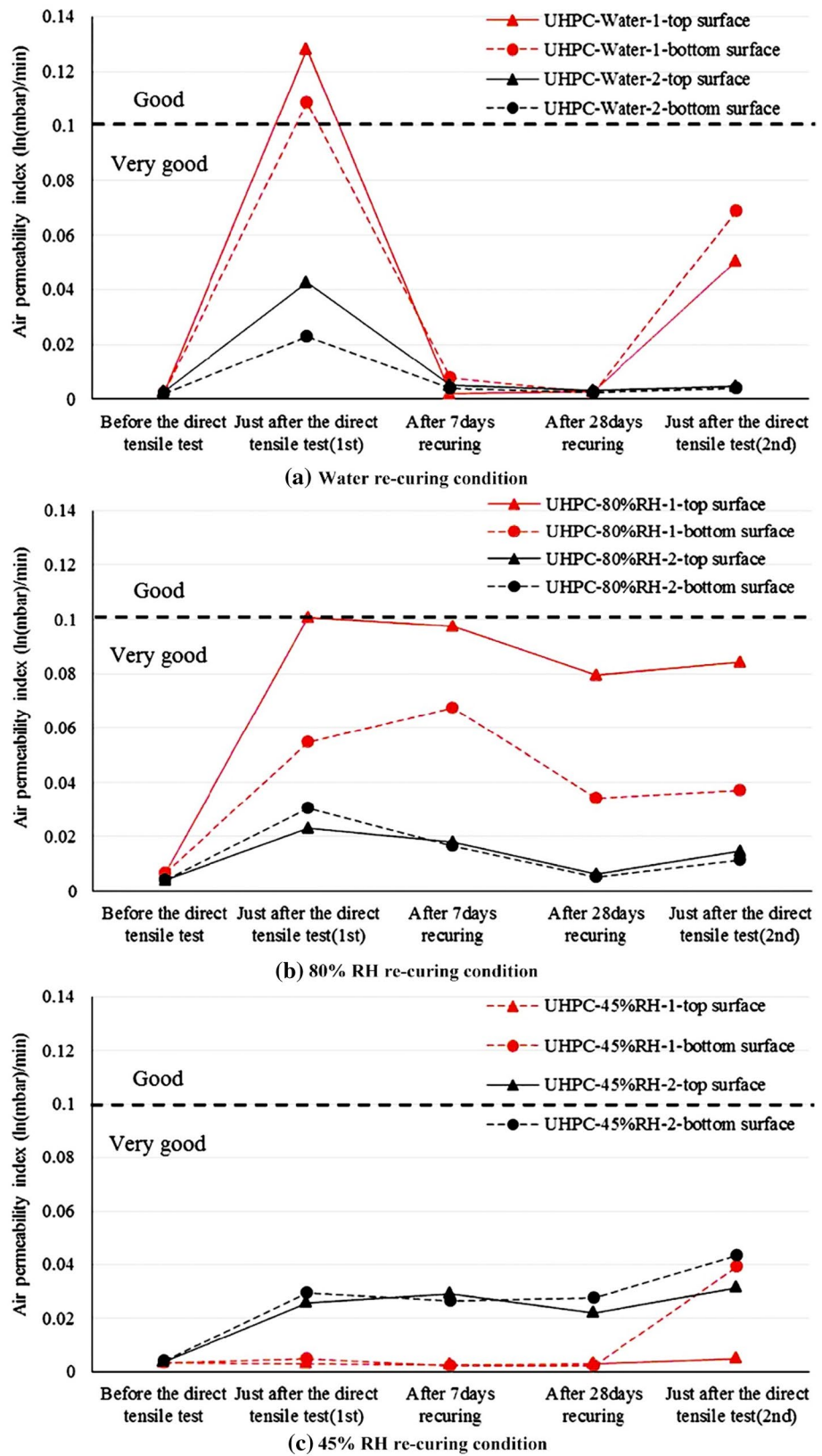
3.3.2 Water permeability

Water permeability is another parameter related to the durability of UHPFRC, relating to the water transferability between the internal pores and external environments. Kunieda et al. [83] adopted the surface penetrant test method to assess the evolution of water penetration resistance of cracked UHPFRC under different loading levels, re-curing conditions, and re-curing periods. Figure 11 shows the setup of the water permeability test. The permeability can be evaluated according to the amount or speed of water infiltrating per unit time, and then the self-healing ability can be evaluated according to the water penetration resistance of the concrete before and after healing.

UHPFRC exhibits superior permeability resistance in uncracked conditions due to its low porosity and denser microstructure [33]. However, the pre-cracking process induces the creation of multi-scale cracks, resulting in higher water permeability. In general, the water permeability is significantly related to the width of induced cracks. Kunieda et al. [83] found that the unloaded strain level (0.1–0.2%) had no significant impact on the recovery of water permeation. That may be contributing to the similar width of cracks between the specimens at 0.1% strain and 0.2% strain. Cracks thinner than 50 μm are considered to have no significant influence on the water permeability of ordinary concrete. The threshold crack opening seems higher for UHPFRC [29], about 130 μm for water permeability coefficient in the study [84], and at least 50 μm in the reference [85].

In contrast to the pre-cracking process, the self-healing process contributes to the increasing insensitivity to water

Fig. 10 Results of air permeability tests [41]



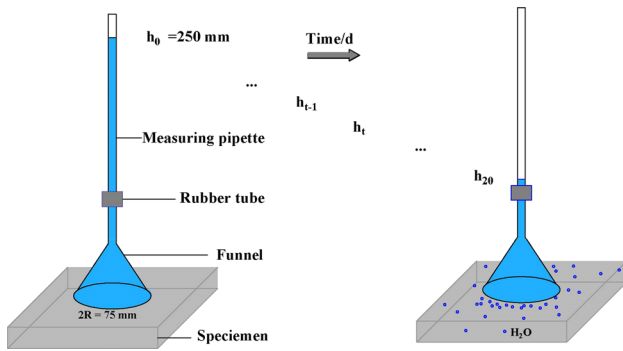


Fig. 11 Outline of the testing method for water permeability, redrawn after Kunieda et al. [83]

penetration of concrete due to the self-healing protection mechanism under proper conditions. In other words, the crack is gradually filled with self-healing products, and the crack width is gradually reduced in the self-healing process. Overall, the external loads coupling with complex environmental effects will slowly weaken the water permeability resistance of UHPFRC, whereas the self-healing will contribute to continuous recovery during the service life, eventually resulting in higher durability.

3.3.3 Chloride penetration

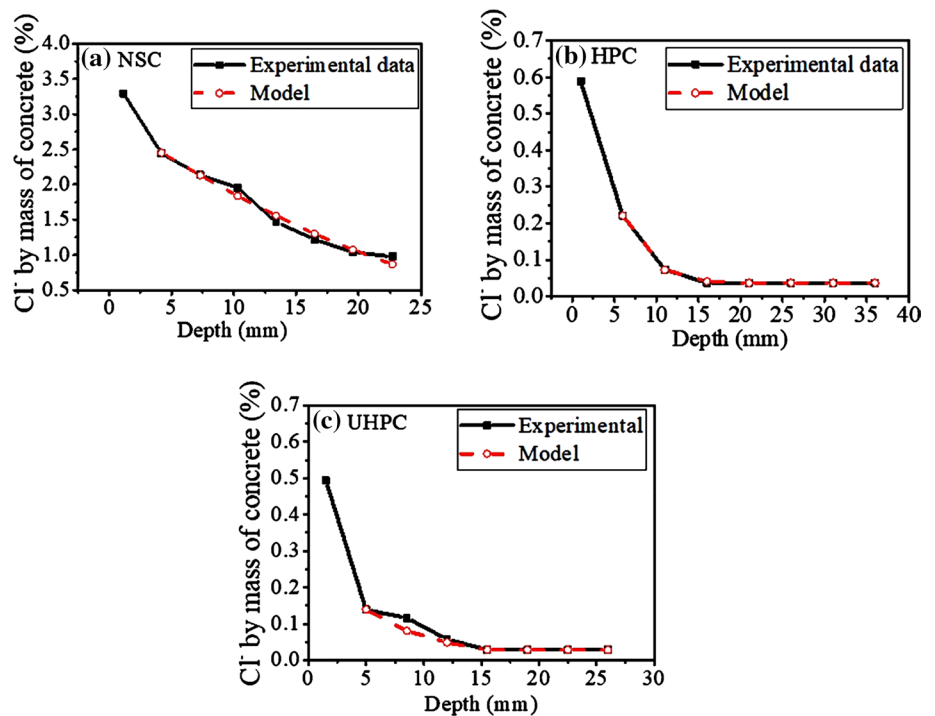
Sohail et al. [86] compared the chloride concentrations in normal strength concrete, high-performance concrete, and UHPC at different depths, as presented in Fig. 12. The

chloride penetration of the UHPC is the slightest, and the tested chloride content is only about 0–0.5% (by mass of concrete), which can be attributed to a denser microstructure with less interconnected pores. Similar conclusions are observed in other literature [33]. Sohail et al. [86] further found a dense formation of C-S-H gel and a smaller interfacial transition zone owing to the pozzolanic reactions of CSMs with portlandite. Like air and water permeability, UHPFRC without any damage also characterizes their extremely weak external ions' transmission capacity due to its low W/B (Fig. 1), dense structure, and discontinuous capillary pores.

However, the chloride permeability resistance will decrease with damage deterioration, especially for the formation of cracks. Hashimoto et al. [87] reported the chloride ion diffusion of UHPFRC with different degrees of damage (crack width = 0, 100 μm, 500 μm, 1000 μm) after being immersed in seawater for three months. With the formation of cracks, the transport depth of chloride ions increased significantly, and its diffusion range increased due to the increased width of the crack. The test results also revealed that the chloride ion penetration only stayed on the initially induced crack surface when the crack width was 100 μm, whereas that became wider in the specimens with a wider crack. Under the external load, the induced cracks and other internal microstructural damage around the cracks provide channels for the transport of ions.

Other studies also demonstrated the effects of cracks on the chloride diffusion of concrete. Cracks harm the resistance against chloride penetration, making it worse for the

Fig. 12 Chloride profiles and curve fitting to calculate the diffusion coefficients: **a** normal strength concrete, **b** high-performance concrete, and **c** UHPC [86]



increasing crack opening, and this phenomenon is consistent in UHPFRC [87]. Meantime, it is widely reported that its effect on chloride penetration is insignificant when the crack width is below a threshold (i.e., critical crack width), as shown in Table 3. The typical test methods of chloride penetration include chloride diffusion (using immersion) and chloride migration (migration cell or rapid chloride migration). The relation between crack depth and crack width was not universally applicable due to the changes in materials and test methods [88]. However, the effects of mixture proportions such as FA content and maximum aggregate size on the chloride diffusion of cracked specimens seem to be negligible [89]. Overall, these results suggest that the closure of cracks induced by self-healing can promote the reduction of chloride diffusion.

Jiang et al. [92] assessed the effects of crack healing on chloride transport using a three-dimensional X-ray microscope and a random walk model. The chloride concentration was decreased with a lower crack width and increased crack self-healing, but no conspicuous change was observed with the change of mixture proportions. Maes et al. [88] indicated that the autogenous self-healing would stabilize chloride penetration when the crack was smaller than 105 μm , while the resistance against the penetration of chlorides would not be much improved for the specimens with more significant cracks. Doostkami et al. [29] assessed the effects of the autogenous self-healing on the permeability to chlorides for pre-cracked UHPFRC. Results indicated that the autogenous healing of UHPFRC is higher than that of conventional concretes for an equivalent total crack. Meantime, many factors contributed to a higher self-healing efficiency, including a low strain level, longer healing time, higher fiber content, and smaller crack size. According to the results of the above literature, cracked UHPFRC can stabilize the penetration of chloride ions in UHPFRC through the self-healing effect. Furthermore, the effect will be more pronounced when the crack is filled with self-healing products until the width is smaller than the critical crack width.

3.3.4 Corrosion resistance

Steel bars or steel fibers are commonly used in UHPFRC structures, and their corrosion will risk the performance of UHPFRC structures. The leading cause of corrosion is the

permeant of chlorides from the surrounding chloride-bearing environment. In other words, a higher chloride penetration resistance will contribute to better anti-corrosion properties, and it can be improved by self-healing of cracks (see Sect. 3.3.3). The resistance against chloride penetration also relates to the material quality (W/C ratio, cement content, impurities), cracks, and the external environments such as moisture, oxygen, humidity, temperature, bacterial attack, and stray currents.

In particular, cracks significantly accelerate the corrosion process of steel fibers in UHPFRC. On the one hand, the fibers inside the sound UHPFRC are challenging to be corroded except for near the exposed surface (0–2 mm), as shown in Fig. 13, but a high steel fiber amount (more than 2%) may lead to an increased risk of electrochemical corrosion [93]. On the other hand, for cracked UHPFRC, the fibers around the cracks are corroded, and the corrosion phenomenon gradually spreads to the fibers in the embedded region [94]. A wider crack will lead to corrosion over a wider area, and worse damages inevitably occur during service life, eventually resulting in the continuous weakening of corrosion resistance and reduction of performance.

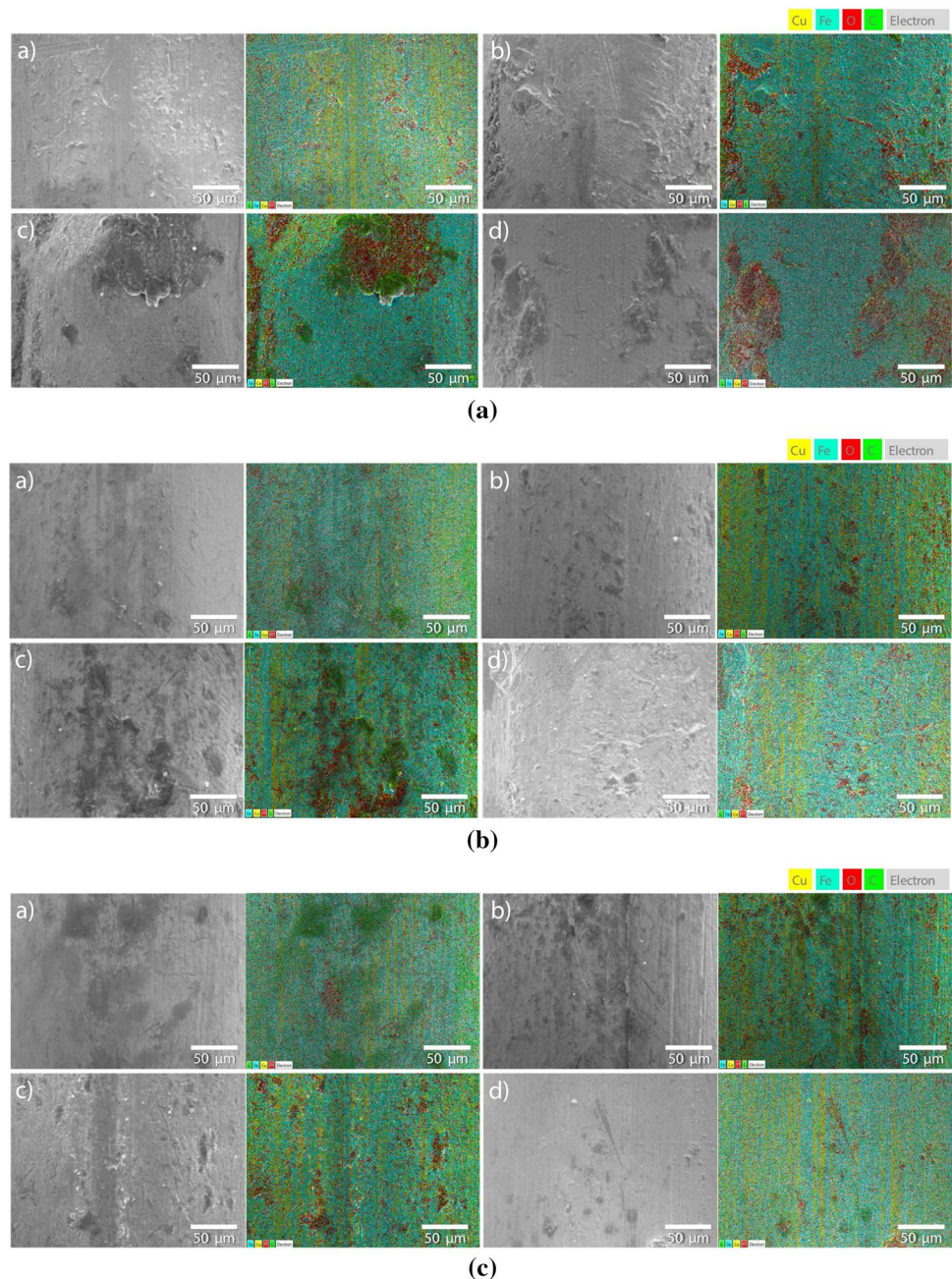
Figure 13 shows the effects of self-healing on the fiber corrosion by mapping the chemical elements on the fiber surface, including the iron (Fe), oxygen (O), carbon (C), and copper (Cu) [23]. The oxygen elements are correlated with the generation of Fe_2O_3 during the corrosion process, and more oxygen elements represent a higher corrosion degree. The author reported that few oxygen elements were detected on the fiber surface in the self-healed specimens. It indicates that fibers are hardly corroded during the self-healing process. In contrast, the corrosion near the exposed surface was evident after exposure to chloride ions and became worse with a longer duration (Fig. 13a). The fibers in cracked specimens will be corroded around cracks, as demonstrated in Sect. 3.3.3. However, the fibers in other locations showed no signs of aggravation of corrosion for the increase of immersed time, behaving with obvious inhibition-effect of the self-healing process on the corrosion (Fig. 13b and c). This phenomenon is consistent with chloride ion penetration in literature [88]. Yoo and Shin [94] also pinpointed that crack repair had a strong inhibitory effect on the steel fiber corrosion in the pre-cracked UHPFRC.

Moreover, the self-healing process is relatively long, and it is difficult to completely suppress the fiber's corrosion around cracks, especially for cracked samples with large initial crack widths. Maes et al. [88] found that the crack healing in larger cracks ($> 105 \mu\text{m}$) would not much improve the resistance against the penetration of aggressive substances such as chlorides due to its uncomplete healing or long time to sealing. The considerably large cracks would lead to severe chloride penetration in concretes, regardless of the inhibition of the self-healing

Table 3 Critical crack width (CCW, μm) for chloride penetration

Types	W/C	Test methods	CCW	Ref
Mortar	0.50	Immersion	10	[88]
Concrete	0.50	Rapid chloride migration testing	12	[90]
Mortar	0.48	Immersion	30	[91]
Concrete	0.40	Steady-state migration test	55–80	[89]

Fig. 13 SEM images and EDS mapping results on pulled fibers from self-healed UHPFRC samples under various NaCl immersion durations: **a** near the exposed surface (2 mm apart), **b** near the exposed surface (5 mm apart), and **c** at the center of cross-section [Note: **a** = self-healed sample and **b**, **c**, and **d** = self-healed samples immersed into NaCl solution for 4, 10, and 20 weeks, respectively [23]



effect, resulting in aggravation of corrosion. Steel fibers will corrode around multiple microcracks due to the penetration of aggressive ions. Moderate corrosion could contribute to a better tensile behavior due to the enhanced fiber-matrix interface, but excessive corrosion would lead to premature fracture of fibers in the cracked UHPFRC [95]. Therefore, in a long-term perspective, the performance of damaged UHPFRC may be deteriorated due to continuous chloride ions penetration and corrosion, and self-healing can play a crucial role in stabilizing corrosion when cracks appear.

4 Mechanism of autogenous self-healing UHPFRC

The self-healing mechanism of UHPFRC cracks can be inspired or referenced from previous studies on the self-healing behavior of concrete or fiber-reinforced concrete based on similarity theory. Pang et al. [96] found that the healing products in concrete cracks mainly consist of CaCO_3 , $\text{Ca}(\text{OH})_2$, calcium-silicate-hydrate, calcium-aluminate-ferrite hydrate, and amorphous silica. The

chemical composition of crack filling materials is complex, especially when the concrete is mixed with various SCMs and other non-traditional components such as superabsorbent polymers. Similarly, these mechanisms were widely recognized or proved in cement-based materials such as strain-hardening cementitious materials [22] and ECC [53]. The autogenous self-healing mechanisms of concrete include physical, mechanical, and chemical causes [63], which can be employed to distinguish the various causes of UHPFRC crack healing.

4.1 Physical and mechanical causes

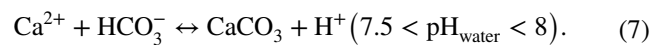
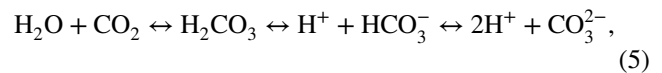
The physical cause of the crack healing is mainly that the cement hydration products near the crack surface expand when exposed to water, and then the crack width becomes smaller, thus playing a beneficial role in blocking water. The expansion of hydrated paste is restricted, which can hardly reduce the liquid flow by more than 10% [63]. Snoeck and Belie [22] reported that superabsorbent polymer near cracks played a beneficial effect on self-healing by absorbed water and swelling. Thus, the addition of water-swellaible substances in hardened UHPFRC may improve the physical impact of self-healing.

Meanwhile, mechanical causes, i.e., the accumulation of fine particles from fracture surface and external environment, tend to promote the self-healing of cracks. However, these causes are considered dispensable for concrete. In particular, better self-healing can be obtained by incorporating more fibers [41] due to an excellent cracking restriction achieved by the bridging and snubbing effects of incorporated fibers in UHPFRC (see Sect. 2.3).

4.2 Chemical causes

The chemical composition of self-healing products is the basis for determining the self-healing mechanism, so

identifications of the crack healing products of UHPFRC have also been carried out in a few works. Kim et al. [2] confirmed the crack filling materials at the crack surfaces to be calcium carbonate (CaCO_3) crystals employing SEM–EDX analysis. Yoo et al. [23] verified the above comment, and the atomic ratio (C: O: Ca) of the new products at a healed crack plane is also similar to that (20: 60: 20) of CaCO_3 . Figure 14 shows the EDS analytical result of particles at the healed crack plane. It can be concluded that the primary healing product is CaCO_3 at the crack surfaces or healed crack plane, and the following Eqs. (5–7) can describe the formation process [97].



Meantime, the self-healing characteristics at different crack positions are not consistent. On the one hand, Jiang et al. [92] reported that the un-hydrated particles at the crack surface first hydrated with water, which contributed to the generation of calcium hydroxide (CH) and calcium-silicate-hydrate (C–S–H) gels. Based on the distribution of healing products, the C–S–H gels did not accumulate in the middle of the cracks but only existed on the surface of the cracks. On the other hand, Fan and Li [53] demonstrated different healing products at different crack depths. The crack surface (from 0 to around 50–150 μm below the surface) can be sealed mainly due to quick crystalline precipitates. In contrast, the continued hydration and pozzolanic reactions may more likely contribute to the formation of healing products at greater depths, with a remarkably long time. Nevertheless, it is not illustrated or demonstrated in recent studies about the self-healing mechanism of UHPFRC.

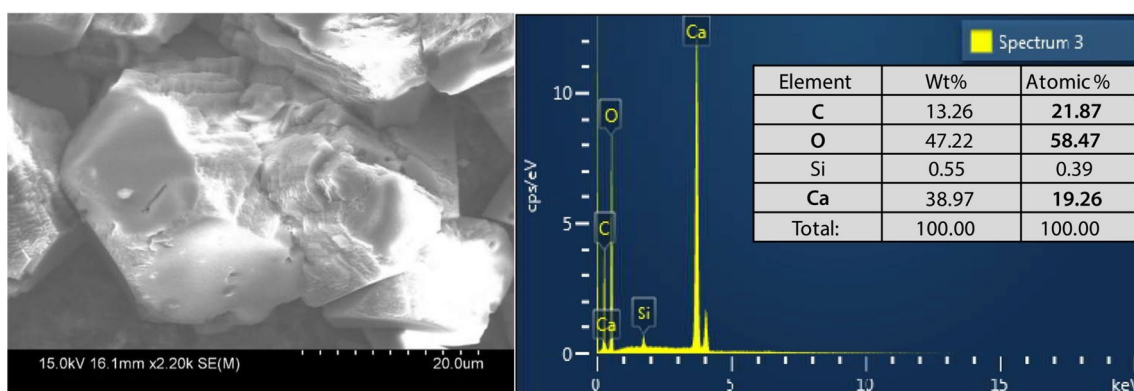


Fig. 14 EDS analytical result on particles at the healed crack plane [23]

Moreover, moderate fibers corrosion promotes performance recovery during the self-healing process. Yoo et al. [23] found that the steel fiber corrosion during the self-healing process can contribute to the higher restoration of tensile performance. With the appearance of microcracks, the steel fibers inside the UHPFRC will corrode due to the entry of external aggressive ions. An increase in the surface roughness of the steel fibers during the self-healing process is relevant to the enhanced tensile performance, which has been confirmed by Atomic force microscopy (AFM) analysis. Yoo et al. [40] also noted that a significant enhancement of pullout resistance of steel fiber in UHPFRC was obtained due to the surface corrosion. The increased interfacial bond between the fiber and matrix led to better tensile performance [98]. Thus, it can be concluded that the partial recovery of tensile performance relates to the improved pullout resistance and bridging capability of fibers by the formation of rust.

5 Summary and outlook

5.1 Summary

Multiple invisible micro-cracks without seasonable processing have an unquestionably negative impact on the long-term performance of UHPFRC, and intrinsic self-healing can timely restrict micro-cracks-induced hazards, which is difficult to resolve through external interventions. This paper reviews the superior potential of autogenous self-healing and its effects on UHPFRC's properties. Based on the review above, the following conclusions can be drawn:

- (1) High potential of autogenous self-healing UHPFRC includes material, hydration, and cracking characteristics: The component of UHPFRC is complicated and flexible, and its proportion is characterized by high binder content (about 943–1542.5 kg/m³), low W/B ratio (about 0.12–0.22), and moderate fiber content (1–3%); Hydration degree of hardened UHPFRC is low (about 30–50%), and its rehydration degree lower than 60% is a large probability event; Visible shrinkage-induced cracks is hardly observed due to the relaxation effect, and high strain-hardening UHPFRC shows outstanding controllability of crack width during the loading process, and the width is typically below 0.05 mm in the strain hardening stage.
- (2) Multi-scale cracks (0–203 μm) in cracked UHPFRC can be wholly or partially sealed during the self-healing process, which significantly depends on the damage degree (i.e., crack width). The width of the full healed crack can reach up to 162 μm after 28 d re-curing in water, and cracks with a width of 75–175 μm showed an excellent self-healing rate or efficiency, which the crack healing kinetics can explain.
- (3) Pre-cracking methods of UHPFRC commonly include a four-point bending test, direct tensile test, uniaxial tensile test, and three points bending test. Thus, correspondingly mechanical properties of UHPFRC (i.e., the strength, first cracking stress, stiffness, toughness, deflection capacity, ductility, etc.) are used to assess the self-healing property. Self-healing can contribute to the recovery of cracked samples, and better performance can be achieved by some methods, e.g., using alumina nanofibers, increasing fiber content, incorporating a crystalline admixture, placing in steam, water, or under high humidity conditions. Moreover, their evolution characteristics have a significant time-dependent effect, i.e., the healing rate is fast at an early age, and the speed drops rapidly with re-curing time.
- (4) A sensible degradation of durability and transport property exists for generating multiple cracks of UHPFRC due to the external loads and transmission of aggressive ions. On the whole, self-healing can achieve a higher performance of UHPFRC by improving the gas permeability resistance, inhibiting the water penetration, stabilizing the penetration of chloride ions, and reducing corrosion. Meantime, the effect of crack width change is considered negligible until the width of cracks in UHPFRC reaches a threshold (at least 50 μm). However, the self-healing protection mechanism is reflected in reducing cracks with larger widths and the complete sealing of micro-scale cracks in UHPFRC.
- (5) Basically, the self-healing of UHPFRC can be partly explained by the mechanisms of autogenous healing concrete, e.g., the further hydration of unreacted cementitious and calcium carbonate formation at the cracks. The healing products mainly are calcium carbonate at the crack surface or healed crack plane in UHPFRC, and the recovery of strength relates to the improved pullout resistance and bridging capability of fibers near the cracks due to the moderate corrosion during the self-healing process.
- (6) Based on the analysis of the self-healing potential and self-healing properties, it is found that there is an obvious non-correspondence. Although UHPFRC can achieve a good self-healing due to the post-crack pattern with multiple microcracks for UHPFRC, the healed maximum crack width is limited after re-curing of 28 days, and it is about 50 μm in most studies, which is much smaller than the 150 μm threshold generally considered for concrete.

5.2 Outlook

The autogenous self-healing property of UHPFRC is prone to solve the problem of microcracks (0–150 μm) in a timely and effective manner, change the traditionally expensive and challenging crack repair mode, and significantly inhibit material deterioration due to cracks during service. Researchers have carried out preliminary research on the self-healing performance of UHPFRC, but there are still many problems to be solved:

- (1) Un-hydrated particles are considered essential components of crack healing reactants for concrete. The self-healing ability of UHPFRC with a high amount of un-hydrated particles has not been effectively improved. Therefore, thoroughly stimulating the unreacted cementitious materials or reducing the cementitious materials through scientific preparation and refined production while realizing the unification of traditional properties with outstanding self-healing properties and carbon emission reduction is one of the future development directions.
- (2) The self-healing process of cracks is affected by many factors. At present, self-healing has a slow healing speed and small crack width that can be completely healed. Research on crack self-healing dynamics and its model and how to accelerate the self-healing process and prevent the deterioration of the substrate at the same time is also one of the future research directions.
- (3) The current research suggests that the performance recovery and crack closure of damaged UHPFRC samples are attributed to crack filling of calcium carbonate crystals and fiber corrosion, while the effects of secondary hydration, ion migration, fiber (especially polar fiber) effect on the self-healing process need to be further studied.
- (4) It is generally believed that it is sufficient when the crack width is less than or equal to the crack width that can fully self-heal. However, the self-healing of cracks relates to the material compositions and application environments. In detail, self-healing is significantly affected by the fiber content, fiber type, binder content, W/C ratio, etc. Meantime, many factors are different in different applications. For example, the characteristics of cracks induced by shrinkage and external loads, the exposure conditions (such as humidity, CO_2 concentration, and temperature), and the healing status (fixed or dynamic loads); Meantime, the current self-healing ability is limited, and it is difficult to achieve complete healing of macroscopic cracks. For non-high strain hardening UHPFRC, more efficient self-healing technology needs to be developed to achieve self-healing of its cracks.

Acknowledgements This study is financially supported by the National Natural Science Foundation of China (Grant Number 52078050). The authors thank the reviewers of this paper for their comments and suggestions and Ms. Yueyang Zhang for her technical support in image processing.

Funding This study was funded by the National Natural Science Foundation of China (Grant Number 52078050).

Declarations

Conflict of interest The authors declare that they have no conflict of interest.

References

1. Yoo D-Y, Kang M-C, Choi H-J, Shin W, Kim S. Influence of chemically treated carbon fibers on the electromagnetic shielding of ultra-high-performance fiber-reinforced concrete. *Arch Civ Mech Eng.* 2020;20:123.
2. Kim S, Yoo D-Y, Kim M-J, Banthia N. Self-healing capability of ultra-high-performance fiber-reinforced concrete after exposure to cryogenic temperature. *Cem Concr Compos.* 2019;104: 103335.
3. Ren L, Fang Z, Wang K. Design and behavior of super-long span cable-stayed bridge with CFRP cables and UHPC members. *Compos Part B-Eng.* 2019;164:72–81.
4. Du J, Meng W, Khayat KH, Bao Y, Guo P, Lyu Z, Abu-obeidah A, Nassif H, Wang H. New development of ultra-high-performance concrete (UHPC). *Compos Part B-Eng.* 2021;224: 109220.
5. Yoo D-Y, Banthia N, Yoon Y-S. Effectiveness of shrinkage-reducing admixture in reducing autogenous shrinkage stress of ultra-high-performance fiber-reinforced concrete. *Cem Concr Compos.* 2015;64:27–36.
6. Guo Y, Yao C, Shen A, Chen Q, Wei Z, Yang X. Feasibility of rapid-regeneration utilization in situ for waste cement-stabilized macadam. *J Clean Prod.* 2020;263: 121452.
7. Lyu Z, Shen A, Meng W. Properties, mechanism, and optimization of superabsorbent polymers and basalt fibers modified cementitious composite. *Constr Build Mater.* 2021;276: 122212.
8. Yao C, Guo Y, Shen A, Cui W, He Z. Recycling of fine-asphalt-pavement solid waste for low-shrinkage rapid hardening Portland cement concrete pavement. *Constr Build Mater.* 2021;289: 123132.
9. Zhang W, Zheng QF, Ashour A, Han BG. Self-healing cement concrete composites for resilient infrastructures: a review. *Compos Part B-Eng.* 2020;189: 107892.
10. Beglarigale A, Vahedi H, Eyice D, Yazici H. Novel test method for assessing bonding capacity of self-healing products in cementitious composites. *J Mater Civil Eng.* 2019;31(4):04019028.
11. Chu H, Jiang L, Xiong C, You L, Xu N. Use of electrochemical method for repair of concrete cracks. *Constr Build Mater.* 2014;73:58–66.
12. Nardi CD, Gardner D, Cazzador G, Cristofori D, Jefferson T. Experimental investigation of a novel formulation of a cyanoacrylate-based adhesive for self-healing concrete technologies. *Front Built Environ.* 2021;7: 660562.
13. White SR, Sottos NR, Geubelle PH, Moore JS, Kessler MR, Sriram SR, Brown EN, Viswanathan S. Autonomic healing of polymer composites. *Nature.* 2001;409:794.
14. Osman KM, Taher FM, Abd El-Tawab A, Faried AS. Role of different microorganisms on the mechanical characteristics, self-healing efficiency, and corrosion protection of concrete under different curing conditions. *J Build Eng.* 2021;41: 102414.

15. Akin A. Investigation of different permeability properties of self-healing cementitious composites under colloidal nano silica curing conditions. *Struct Concr.* 2021;9:1–14.
16. Sahmaran M, Yildirim G, Noori R, Ozbay E, Lachemi M. Repeatability and pervasiveness of self-healing in engineered cementitious composites. *ACI Mater J.* 2015;112:513–22.
17. Xue CH, Li WG, Luo ZY, Wang KJ, Castel A. Effect of chloride ingress on self-healing recovery of smart cementitious composite incorporating crystalline admixture and MgO expansive agent. *Cem Concr Res.* 2021;139: 106252.
18. Garces JIT, Dollente IJ, Beltran AB, Tan RR, Promentilla MAB. Life cycle assessment of self-healing geopolymer concrete. *Clean Eng Technol.* 2021;4: 100147.
19. Park B, Choi YC. Investigating a new method to assess the self-healing performance of hardened cement pastes containing supplementary cementitious materials and crystalline admixtures. *J Mater Res Technol.* 2019;8:6058–73.
20. Snoeck D, De Belie N. From straw in bricks to modern use of microfibers in cementitious composites for improved autogenous healing—a review. *Constr Build Mater.* 2015;95:774–87.
21. Calvo JLG, Perez G, Carballosa P, Erkizia E, Gaitero JJ, Guerrero A. Development of ultra-high performance concretes with self-healing micro/nano-additions. *Constr Build Mater.* 2017;138:306–15.
22. Snoeck D, Belie ND. Autogenous healing in strain-hardening cementitious materials with and without superabsorbent polymers: an 8-year study. *Fron Mater.* 2019;6:48.
23. Yoo DY, Shin W, Chun B, Banthia N. Assessment of steel fiber corrosion in self-healed ultra-high-performance fiber-reinforced concrete and its effect on tensile performance. *Cem Concr Res.* 2020;133: 106091.
24. Granger S, Loukili A, Pijaudier-Cabot G, Chanvillard G. Mechanical characterization of the self-healing effect of cracks in ultra high performance concrete. In: proceedings third international conference on construction materials, performance, innovations and structural implications, vancouver. 2005;pp. 22–24.
25. Zhu H, Zhang D, Wang TY, Wu HL, Li VC. Mechanical and self-healing behavior of low carbon engineered cementitious composites reinforced with PP-fibers. *Constr Build Mater.* 2020;259: 119805.
26. Ozbay E, Sahmaran M, Lachemi M, Yucel HE. Self-healing of microcracks in high-volume fly-ash-incorporated engineered cementitious composites. *ACI Mater J.* 2013;110:32–42.
27. Ozbay E, Sahmaran M, Yucel HE, Erdem TK, Lachemi M, Li VC. Effect of sustained flexural loading on self-healing of engineered cementitious composites. *J Adv Concr Technol.* 2013;11:167–79.
28. Ferrara L, Krelani V, Moretti F, Roig Flores M, Serna RP. Effects of autogenous healing on the recovery of mechanical performance of High Performance Fibre Reinforced Cementitious Composites (HPFRCCs): part 1. *Cem Concr Compos.* 2017;83:76–100.
29. Doostkami H, Roig-Flores M, Serna P. Self-healing efficiency of Ultra High-Performance Fiber-Reinforced Concrete through permeability to chlorides. *Constr Build Mater.* 2021;310: 125168.
30. Shi CJ, Wu ZM, Xiao JF, Wang DH, Huang ZY, Fang Z. A review on ultra high performance concrete: Part I. Raw materials and mixture design. *Constr Build Mater.* 2015;101:741–51.
31. Yoo DY, Yoon YS. A review on structural behavior, design, and application of ultra-high-performance fiber-reinforced concrete. *Int J Concr Struct Mater.* 2016;10:125–42.
32. Shaikh FUA, Luhar S, Arel HS, Luhar I. Performance evaluation of Ultrahigh performance fibre reinforced concrete—a review. *Constr Build Mater.* 2020;232: 117152.
33. Li JQ, Wu ZM, Shi CJ, Yuan Q, Zhang ZH. Durability of ultra-high performance concrete—a review. *Constr Build Mater.* 2020;255: 119296.
34. Xue JQ, Briseghella B, Huang FY, Nuti C, Tabatabai H, Chen BC. Review of ultra-high performance concrete and its application in bridge engineering. *Constr Build Mater.* 2020;260: 119844.
35. Sahmaran M, Yildirim G, Erdem TK. Self-healing capability of cementitious composites incorporating different supplementary cementitious materials. *Cem Concr Compos.* 2013;35:89–101.
36. Yildirim G, Khiavi AH, Yesilmen S, Sahmaran M. Self-healing performance of aged cementitious composites. *Cem Concr Compos.* 2018;87:172–86.
37. Cuenca E, Ferrara L. Self-healing capacity of fiber reinforced cementitious composites. State of the art and perspectives. *KSCE J Civ Eng.* 2017;21:2777–89.
38. Pourjahanshahi A, Madani H. Chloride diffusivity and mechanical performance of UHPC with hybrid fibers under heat treatment regime. *Mater Today Commun.* 2021;26:102146.
39. Cuenca E, Ambrosio LD, Lizunov D, Tretjakov A, Volobujeva O, Ferrara L. Mechanical properties and self-healing capacity of Ultra High Performance Fibre Reinforced Concrete with alumina nano-fibres: Tailoring Ultra High Durability Concrete for aggressive exposure scenarios. *Cem Concr Compos.* 2021;118:103956
40. Yoo DY, Gim JY, Chun B. Effects of rust layer and corrosion degree on the pullout behavior of steel fibers from ultra -high-performance concrete. *J Mater Res Technol.* 2020;9:3632–48.
41. Guo JY, Wang JY, Wu K. Effects of self-healing on tensile behavior and air permeability of high strain hardening UHPC. *Constr Build Mater.* 2019;204:342–56.
42. Hajiesmaeili A, Hafiz MA, Denarié E. Tensile response of Ultra High Performance PE Fiber Reinforced Concretes (PE-UHPFRC) under imposed shrinkage deformations. *Mater Struct.* 2021;54:114.
43. Hajiesmaeili A, Denarié E. Capillary flow in UHPFRC with synthetic fibers, under high tensile stresses. *Cem Concr Res.* 2021;143: 106368.
44. Yu R, Spiesz P, Brouwers HJH. Mix design and properties assessment of Ultra-High Performance Fibre Reinforced Concrete (UHPFRC). *Cem Concr Res.* 2014;56:29–39.
45. Cuenca E, Serna P. Autogenous self-healing capacity of early-age ultra-high-performance fiber-reinforced concrete. *Sustainability.* 2021;13:3061.
46. Huang H, Gao X, Khayat KH. Contribution of fiber orientation to enhancing dynamic properties of UHPC under impact loading. *Cem Concr Compos.* 2021;121: 104108.
47. Wu Z, Khayat KH, Shi C, Tutikian BF, Chen Q. Mechanisms underlying the strength enhancement of UHPC modified with nano-SiO₂ and nano-CaCO₃. *Cem Concr Compos.* 2021;119: 103992.
48. Niu Y, Wei J, Jiao C. Crack propagation behavior of ultra-high-performance concrete (UHPC) reinforced with hybrid steel fibers under flexural loading. *Constr Build Mater.* 2021;294: 123510.
49. Akhnouk AK, Buckhalter C. Ultra-high-performance concrete: constituents, mechanical properties, applications and current challenges. *Case Stud Constr Mat.* 2021;15: e00559.
50. Isa MN, Pilakoutas K, Guadagnini M, Angelakopoulos H. Mechanical performance of affordable and eco-efficient ultra-high performance concrete (UHPC) containing recycled tyre steel fibres. *Constr Build Mater.* 2020;255: 119272.
51. Guan XC, Zhang CC, Li YZ, Zhao SY. Effect of exposure conditions on self-healing behavior of engineered cementitious composite incorporating limestone powder. *Cem Concr Compos.* 2020;114: 103808.
52. Siad H, Alyousif A, Keskin OK, Keskin SB, Lachemi M, Sahmaran M, Hossain KMA. Influence of limestone powder on mechanical, physical and self-healing behavior of Engineered Cementitious Composites. *Constr Build Mater.* 2015;99:1–10.

53. Fan S, Li M. X-ray computed microtomography of three-dimensional microcracks and self-healing in engineered cementitious composites. *Smart Mater Struct.* 2015;24: 015021.
54. Li Y, Li J, Yang E-H, Guan X. Investigation of matrix cracking properties of engineered cementitious composites (ECCs) incorporating river sands. *Cem Concr Compos.* 2021;123: 104204.
55. Allahyari H, Heidarpour A, Shayan A. Experimental and analytical studies of bacterial self-healing concrete subjected to alkali-silica-reaction. *Constr Build Mater.* 2021;310: 125149.
56. Nili M, Ramezani-pour AA, Sobhani J. Evaluation of the effects of silica fume and air-entrainment on deicer salt scaling resistance of concrete pavements: microstructural study and modeling. *Constr Build Mater.* 2021;308: 124972.
57. Wang J, Sun H, Yu L, Liu S, Geng D, Yuan L, Zhou Z, Cheng X, Du P. Improvement of intrinsic self-healing ability of concrete by adjusting aggregate gradation and sand ratio. *Constr Build Mater.* 2021;309: 124959.
58. Aspiotis K, Sotiriadis K, Ntaska A, Mácová P, Badogiannis E, Tsivilis S. Durability assessment of self-healing in ordinary Portland cement concrete containing chemical additives. *Constr Build Mater.* 2021;305: 124754.
59. Rauf M, Khaliq W, Khushnood RA, Ahmed I. Comparative performance of different bacteria immobilized in natural fibers for self-healing in concrete. *Constr Build Mater.* 2020;258: 119578.
60. Singh H, Gupta R. Influence of cellulose fiber addition on self-healing and water permeability of concrete. *Case Stud Constr Mat.* 2020;12: e00324.
61. Larrard F, Sedran T. Optimization of ultra-high-performance concrete by the use of a packing model. *Cem Concr Res.* 1994;24:997–1009.
62. Mishra O, Singh SP. An overview of microstructural and material properties of ultra-high-performance concrete. *J Sustain Cement-Based Mater.* 2019;8:97–143.
63. Rooij M, Tittelboom KV, Belie ND, Schlangen E. Self-healing phenomena in cement-based materials. Dordrecht: Springer; 2013.
64. An MJ, Liu YZ, Zhang G, Wang Y, Yu ZR. Influence of rehydration effect on microstructure and water stability of ultra-high performance concrete matrix. *J Chin Ceram Soc.* 2020;48:1722–31 (in Chinese).
65. Granger S, Loukili A, Pijaudier-Cabot G, Chanvillard G. Experimental characterization of the self-healing of cracks in an ultra high performance cementitious material: mechanical tests and acoustic emission analysis. *Cem Concr Res.* 2007;37:519–27.
66. Huang H, Ye G. Simulation of self-healing by further hydration in cementitious materials. *Cem Concr Compos.* 2012;34:460–7.
67. Park JJ, Yoo DY, Kim SW, Yoon YS. Drying shrinkage cracking characteristics of ultra-high-performance fibre reinforced concrete with expansive and shrinkage reducing agents. *Mag Concr Res.* 2013;65:248–56.
68. Yoo D-Y, Park J-J, Kim S-W, Yoon Y-S. Influence of reinforcing bar type on autogenous shrinkage stress and bond behavior of ultra high performance fiber reinforced concrete. *Cem Concr Compos.* 2014;48:150–61.
69. Hafiz MA, Hajiesmaeili A, Denarié E. Tensile response of low clinker UHPFRC subjected to fully restrained shrinkage. *Cem Concr Res.* 2019;124: 105804.
70. Yoo DY, Park JJ, Kim SW, Yoon YS. Combined effect of expansive and shrinkage-reducing admixtures on the properties of ultra high performance fiber-reinforced concrete. *J Compos Mater.* 2014;48:1981–91.
71. Habel K, Charron J-P, Denarié E, Brühwiler E. Autogenous deformations and viscoelasticity of UHPFRC in structures. Part I: experimental results. *Mag Concr Res.* 2006;58:135–45.
72. Yoo D-Y, Min K-H, Lee J-H, Yoon Y-S. Shrinkage and cracking of restrained ultra-high-performance fiber-reinforced concrete slabs at early age. *Constr Build Mater.* 2014;73:357–65.
73. Wang J-Y, Guo J-Y. Damage investigation of ultra high performance concrete under direct tensile test using acoustic emission techniques. *Cem Concr Compos.* 2018;88:17–28.
74. Wille K, El-Tawil S, Naaman AE. Properties of strain hardening ultra high performance fiber reinforced concrete (UHP-FRC) under direct tensile loading. *Cem Concr Compos.* 2014;48:53–66.
75. Yoo D-Y, Banthia N, Yoon Y-S. Flexural behavior of ultra-high-performance fiber-reinforced concrete beams reinforced with GFRP and steel rebars. *Eng Struct.* 2016;111:246–62.
76. Luo J, Shao X, Fan W, Cao J, Deng S. Flexural cracking behavior and crack width predictions of composite (steel + UHPC) light-weight deck system. *Eng Struct.* 2019;194:120–37.
77. Qiu M, Shao X, Zhu Y, Zhan J, Wang Y. Experimental investigation on flexural cracking behavior of ultrahigh performance concrete beams. *Struct Concr.* 2020;21:2134–53.
78. Snoeck D, De Belie N. Mechanical and self-healing properties of cementitious composites reinforced with flax and cottonised flax, and compared with polyvinyl alcohol fibres. *Biosyst Eng.* 2012;111:325–35.
79. Nishiwaki T, Kwon S, Homma D, Yamada M, Mihashi H. Self-healing capability of fiber-reinforced cementitious composites for recovery of watertightness and mechanical properties. *Materials.* 2014;7:2141–54.
80. Gagne R, Argouges M. A study of the natural self-healing of mortars using air-flow measurements. *Mater Struct.* 2012;45:1625–38.
81. Wang XF, Fang C, Li DW, Han NX, Xing F. A self-healing cementitious composite with mineral admixtures and built-in carbonate. *Cem Concr Compos.* 2018;92:216–29.
82. Zhang D, Li K. Concrete gas permeability from different methods: correlation analysis. *Cem Concr Compos.* 2019;104: 103379.
83. Kunieda M, Choonghyun K, Ueda N, Nakamura H. Recovery of protective performance of cracked ultra high performance-strain hardening cementitious composites (UHP-SHCC) due to autogenous healing. *J Adv Concr Technol.* 2012;10:313–22.
84. Charron JP, Denarié E, Brühwiler E. Permeability of ultra high performance fiber reinforced concretes (UHPFRC) under high stresses. *Mater Struct.* 2007;40:269–77.
85. Negrini A, Roig-Flores M, Mezquida-Alcaraz EJ, Ferrara L, Serna P. Effect of crack pattern on the self-healing capability in traditional, HPC and UHPFRC concretes measured by water and chloride permeability. In: 7th International Conference on Concrete Repair, Cluj Napoca, Romania. 2019;pp. 1–8.
86. Sohail MG, Kahraman R, Al Nuaimi N, Gencturk B, Alnahhal W. Durability characteristics of high and ultra-high performance concretes. *J Build Eng.* 2021;33:1011669.
87. Hashimoto K, Toyoda T, Yokota H, Kono T, Kawaguchi T. Tension-softening behavior and chloride ion diffusivity of cracked ultra high strength fiber reinforced concrete. RILEM-Fib-AFGC International Symposium on Ultra High Performance Fibre-Reinforced Concrete, Marseille, France. 2014;pp. 257–64.
88. Maes M, Snoeck D, De Belie N. Chloride penetration in cracked mortar and the influence of autogenous crack healing. *Constr Build Mater.* 2016;115:114–24.
89. Jang SY, Kim BS, Oh BH. Effect of crack width on chloride diffusion coefficients of concrete by steady-state migration tests. *Cem Concr Res.* 2011;41:9–19.
90. Yoon IS, Schlangen E, Rooij M, Breugel KV. The effect of cracks on chloride penetration into concrete. *Key Eng Mater.* 2007;348–349:769–72.
91. Ismail M, Toumi A, François R, Gagné R. Effect of crack opening on the local diffusion of chloride in cracked mortar samples. *Cem Concr Res.* 2008;38:1106–11.
92. Jiang J, Zheng X, Wu S, Liu Z, Zheng Q. Nondestructive experimental characterization and numerical simulation on self-healing and chloride ion transport in cracked ultra-high performance concrete. *Constr Build Mater.* 2019;198:696–709.

93. Song Q, Yu R, Shui Z, Rao S, Wang X, Sun M, Jiang C. Steel fibre content and interconnection induced electrochemical corrosion of Ultra-High Performance Fibre Reinforced Concrete (UHPFRC). *Cem Concr Compos.* 2018;94:191–200.
94. Yoo D-Y, Shin W. Improvement of fiber corrosion resistance of ultra-high-performance concrete by means of crack width control and repair. *Cem Concr Compos.* 2021;121: 104073.
95. Shin W, Yoo D-Y. Influence of steel fibers corroded through multiple microcracks on the tensile behavior of ultra-high-performance concrete. *Constr Build Mater.* 2020;259: 120428.
96. Pang B, Zhou Z, Hou P, Du P, Zhang L, Xu H. Autogenous and engineered healing mechanisms of carbonated steel slag aggregate in concrete. *Constr Build Mater.* 2016;107:191–202.
97. Edvardsen C. Water permeability and autogenous healing of cracks in concrete. *ACI Mater J.* 1999;96:448–54.
98. Nguyễn HH, Choi J-I, Kim H-K, Lee BY. Effects of the type of activator on the self-healing ability of fiber-reinforced alkali-activated slag-based composites at an early age. *Constr Build Mater.* 2019;224:980–94.